ORIGINAL ARTICLE

Computer-assisted distraction osteogenesis by Ilizarov's method

A. L. Simpson[1,4]
B. Ma[4]
B. Slagel[2,4]
D. P. Borschneck[2,4]
R. E. Ellis[1,2,3,4]*

[1]*School of Computing, Queen's University, Kingston, ON, Canada*

[2]*Department of Surgery, Queen's University, Kingston, ON, Canada*

[3]*Department of Mechanical Engineering, Queen's University, Kingston, ON, Canada*

[4]*Human Mobility Research Centre, Kingston General Hospital, Kingston, ON, Canada*

*Correspondence to: R. E. Ellis, School of Computing, Queen's University, Kingston, Ontario K7L 3N6, Canada.
E-mail: ellis@cs.queensu.ca

Abstract

Background   The Taylor spatial frame is a fixation device used to implement the Ilizarov method of bone deformity correction to gradually distract an osteotomized bone at regular intervals, according to a prescribed schedule.

Methods   We modify conventional technique by: (a) preoperatively planning a virtual three-dimensional (3D) correction; (b) basing the correction on the actual location of the frame with respect to the anatomy, immediately compensating for frame mounting errors; and (c) calculating the correction based on 3D CT data rather than measurements from radiographs. We have performed a laboratory study using plastic phantoms, and a pilot clinical study involving five patients.

Results   In 20 tibial phantom experiments, we achieved average correction errors of $<2°$ total rotation and <0.5 mm total lengthening. We observed clinically acceptable corrections with no complications in our pilot clinical study.

Conclusions   Our method achieved high accuracy and precision in a laboratory setting, and produced acceptable outcomes in a pilot clinical study. Copyright © 2008 John Wiley & Sons, Ltd.

Keywords   computer-assisted surgery; orthopaedic surgery; Ilizarov technique; distraction osteogenesis

Introduction

Rotational and translational deformities in the long bones can be corrected using distraction osteogenesis, developed by Russian orthopaedic surgeon Gavril Ilizarov. Ilizarov's method is based on the biological principle of inducing new bone growth by gradually distracting a fracture at regular intervals. More specifically, the method is achieved by performing a corticotomy or osteotomy on the deformed bone, fixating the distressed bone with a mechanical fixator, and distracting the bone according to a set schedule of corrections. Ilizarov's method has been successfully used for limb lengthening, limb reconstruction, limb salvage, fracture management, treatment of osteomyelitis, angular deformities, non-unions and malunions (1–3).

The Taylor spatial frame, which we describe in greater detail in Section 1.1, is one type of Ilizarov fixator. Conventional surgical technique for this fixator is subject to two sources of error: (a) preoperatively planning the required correction requires the precise measurement of 13 parameters from clinical

examination and radiographs; and (b) angular and translational errors may be present if the frame is mounted such that it does not accurately mimic the deformity.

We have developed a computer-assisted technique that modifies the conventional approach to deformity correction, using the Ilizarov method in four fundamental ways:

1. The need for the surgeon to preoperatively compute the frame parameters is removed.
2. The performed correction is based on the actual location of the frame with respect to the anatomy; any translational or angular malalignments that occur while mounting the frame are compensated for immediately, thereby potentially removing the need for residual correction.
3. The correction is calculated based on 3D coordinates from CT data, rather than measured from radiographs.
4. The surgeon has flexibility in frame placement; hence, anatomical constraints that may not have been apparent preoperatively can be compensated for in surgery.

The Taylor spatial frame

The Taylor spatial frame (Smith & Nephew, Memphis, TN, USA) is an external fixator that consists of six telescopic rods (called struts) connecting two circular bases (or rings). By adjusting the lengths of the struts, the rings move with respect to each other. Adjusting the strut lengths can reproduce a wide range of deformities. The frame is adjusted postoperatively by the patient according to a prescribed schedule of corrections. Figure 1 shows the Taylor spatial frame before and after adjustment of the struts.

In the conventional technique, the surgeon sets and measures 13 parameters preoperatively from plain X-rays and in the clinic. The 13 parameters are used by a computer program – supplied by the manufacturer of the frame – to generate the six specific strut lengths and the correction schedule for the frame. The frame is then surgically mounted to the patient. The patient adjusts the frame each day according to the correction schedule (4).

More specifically, the surgeon determines the correction and 13 frame parameters preoperatively. The 13 parameters are (5):

- Three rotational and three translational parameters that describe the anteroposterior angulation, mediolateral angulation and axial angulation, measured using plain film X-ray and physical examination.
- Three frame parameters that specify the two ring diameters and neutral frame height.
- Four parameters that describe the location and axial rotation of the reference bone fragment with respect to the reference ring.

The Taylor spatial frame is kinematically equivalent to the Stewart platform, which is fully coupled (6); hence, changing the length of any one strut results in a six-degree-of-freedom change in the configuration of the frame.

There are two primary methods of surgically mounting the Taylor spatial frame (5) for treatment of malunions or congenital deformities; additional methods are available for treatment of acute fractures. In the chronic-deformity correction method, the struts of the assembled spatial frame are adjusted so that the frame mimics the deformity; the strut lengths are computed based on the 13 frame parameters using a software program. The surgeon attaches the frame to the patient so that the frame matches the nature of the deformity; the deformity is
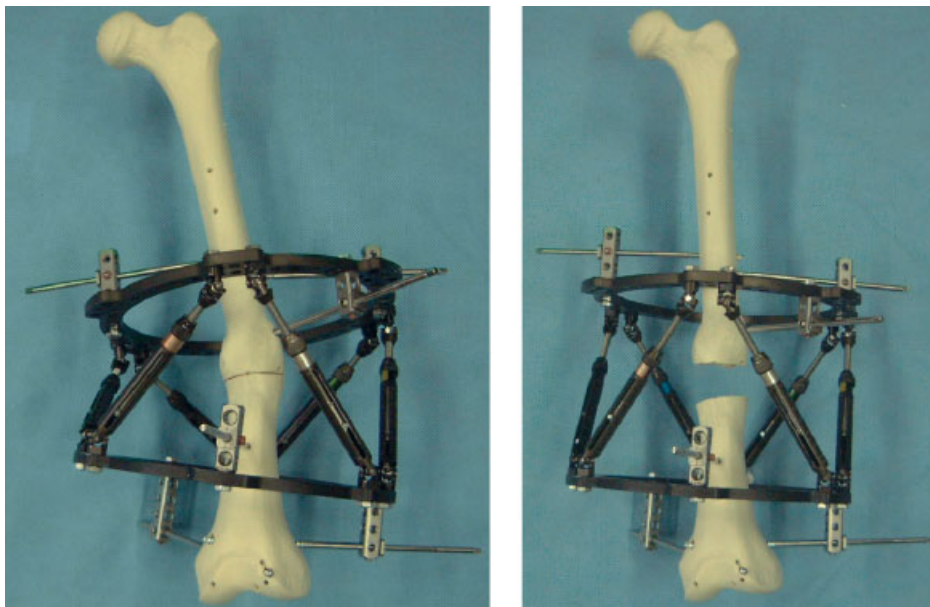

Figure 1. (Left) The deformed Taylor spatial frame before correction. (Right) The neutral Taylor spatial frame after correction

fully corrected once the frame reaches its neutral shape, with all six struts having equal length. Alternatively, the rings-first method of deformity correction mounts the rings to the patient prior to attaching the struts. The rings are mounted perpendicular to the distal and proximal ends of the bone, and the struts are attached to the frame. The deformity is corrected when the frame is returned to its neutral shape with the correct frame height.

In both primary methods, the surgeon mounts the rings approximately perpendicular to the weight-bearing axis of the limb under fluoroscopic guidance, using either Steinman pins or flexible tensioned Kirschner wires. The surgeon simulates a bone fracture by performing a corticotomy or osteotomy and mounts the frame to the patient in the configuration prescribed by the software. The patient adjusts the struts according to the schedule of corrections, which is calculated by the software. When the schedule is complete and the frame is in its neutral position, any residual deformity is corrected by applying a secondary correction schedule. According to Taylor and Paley, this residual-correction phase is usually required to correct accumulated errors (4).

Both the chronic deformity-correction and rings-first methods assume that the frame accurately mimics the deformity when it is first mounted to the patient. If there are measurement errors in the frame parameters or procedural errors in mounting the frame, then there will some residual error when the frame is returned to its neutral shape and height. The residual-deformity correction and total-residual-deformity correction methods compensate for any residual deformity which may exist after either of the first two methods is used. The residual-deformity correction method is used when there is a remaining deformity after the frame is returned to its neutral configuration. The total-residual deformity correction method can be used even when the frame is not in its neutral configuration; Taylor (5) refers to this situation as 'the problem of a crooked bone in a differently crooked frame'. Both methods require the reassessment of most of the frame parameters.

Related work

Rajacich and colleagues observed that a single point of failure in performing the Ilizarov method is planning the procedure (9). In the case of the Taylor spatial frame, 13 frame parameters must be measured from the patient and radiographs. Measurement error in any one parameter will propagate through the entire preoperative plan, likely resulting in a residual deformity. A second source of error is the misapplication of the frame, such that translational and angular problems are introduced during surgery.

Seide and colleagues described a hexapod fixator that, like the Taylor frame, was based on a Stewart platform. A study using 16 consecutive patients treated with a manually adjusted fixator was reported (7). Reasons for surgery were: displaced tibial fractures; deformities after treatment of tibial fractures; and axial deformity after tibial lengthening. Rotational deformities up to 35° and translational displacements up to 40 mm were treated. They reported a 9° correction error in one case that was caused by misinterpretation of the radiographs. More recently, the authors have described a motorized version of their fixator (8), where the shape of the fixator was controlled by a computer driving linear motors on each strut. They alluded to surgical navigation being a possibility.

Feldman and colleagues (2) reported on a consecutive series of 18 cases of tibial mal-union and non-union treated with the Taylor spatial frame; 17 of the 18 patients ultimately achieved total angular correction no worse than 3.6° and translational correction no worse than 3 mm. Seven patients required residual deformity correction; the authors speculated that the cause may have been loss of stiffness in the wires or errors in calculating the frame parameters. They reported that the need for residual correction was higher in larger deformities and during their learning curve phase.

Fadel and Hosny (10) reported on 22 cases of lower limb deformity correction using the Taylor spatial frame. Two cases failed to achieve the desired correction, one of which was attributed to an inaccurate initial assessment.

In a conference proceedings, we described a small study comparing six traditional to six of our computer-assisted Taylor spatial frame corrections of a deformed plastic tibia (11). A normal version of the same tibia was used to determine the ground-truth correction. The traditional method produced a mean correction error of 5.5° (1° standard deviation), and our computer-assisted method produced a mean correction error of 1.6° (0.7° standard deviation).

Early work by Kochs (12) attempted to reduce complications of the frame due to incorrect preoperative planning and inaccurate application by simulating the planned correction. Optimal joint positions and ring locations were obtained by simulation on images acquired from hand-tracing radiographs and scanning these images. Postoperatively, a radiograph was compared to the preoperative plan to determine the necessary residual corrections. Lin *et al.* (13) proposed a preoperative planning system for the Ilizarov method that created a bone template using an ultrasonic digitizer, manually characterized the deformity from radiographs and patient examination, and performed a virtual osteotomy on the template. The frame was assembled using a life-size diagram of the fixator assembly output by the computer. In both methods, the correction is calculated from radiographs rather than 3D coordinates from CT data.

More recently, Iyun and colleagues (14) applied the inverse kinematics of the Taylor spatial frame to the final (neutral) configuration of the frame to derive the initial (deformed) configuration. The placement of the Steinman pins was determined preoperatively and guided intraoperatively. Their methodology had two impractical assumptions. The first and most significant assumption was that the frame is always mounted using rigid pins,

which is not the case when a ring must be mounted close to a joint line using Kirshner wires. The second assumption was that the location and direction of the fixation pins could be determined during the planning phase. In practice, the configuration of the wires, pins and Rancho cubes (used to attach the wires or pins to the frame) are best chosen intraoperatively because of anatomical constraints that may not be apparent preoperatively. The results of the laboratory study were limited by a learning effect present in the results; once the surgeon mounted the first frame in the conventional manner; subsequent frames were mounted without error.

Our approach

The major sources of error when using the Taylor frame are measuring the frame parameters, planning the 3D correction based on radiographs and clinical examination, and intraoperatively mounting the frame to the patient so that it accurately mimics the deformity. We aim to minimize the effects of these errors by: preoperatively planning the correction using 3D CT data; intraoperatively measuring the position and orientation of the frame relative to the bony anatomy; and postoperatively computing an appropriate correction schedule.

We perform preoperative planning using 3D models rendered from the CT dataset. The 3D models allow the surgeon to visualize and understand the deformity. If desired, a physical replica of the deformed bone can be produced using rapid prototyping technology. If the deformity is unilateral, then a model of the unaffected limb can be used as a template to guide the correction. We believe that planning in 3D allows for a more accurate assessment of the six parameters describing the deformity.

The four parameters describing the relationship between the reference ring and bone fragment are determined by registering the patient and the rings to the CT coordinate system. The registration transformations yield the initial (immediate postoperative) configuration of the rings in CT coordinates, and the preoperative plan gives the final configuration of the rings; hence, an appropriate correction schedule can be computed without the need to accurately mount the frame to the patient. The neutral frame height parameter is not required by our approach. In the remainder of this paper, we present our detailed methodology, demonstrate the improvement of our technique over the traditional approach in a study of 20 phantoms, and discuss five of our clinical procedures. This article is an expanded version of work previously published in two conference proceedings, wherein we described the results of a smaller laboratory study (15) and a single patient case study (16).

Materials and methods

Our technique consisted of three phases (A–C) divided into a total of eight major steps (plus one additional validation step used in our laboratory study). Technical details can be found in the Appendix. In summary, our technique was:

A: Preoperative phase

A1: *Patient care*. Preoperative patient care was the same as for conventional technique. Clinical assessment of the magnitude of the deformity angles was performed to aid in planning, even though a CT scan would later be performed.

A2: *CT scan*. A CT scan of the target anatomy was obtained, from which a 3D surface model was computed.

A3: *Preoperative planning*. A preoperative plan was created using custom software developed at our institution. First, a virtual osteotomy was performed by cutting the model into two fragments; we represented the distal fragment as fixed and the proximal fragment as mobile. Next, a reference point on the distal fragment was selected (usually at the geometric centre of the cut surface of the distal model). Finally, a virtual correction was performed by rotating and translating the proximal fragment into the desired position. An example plan using the unaffected contralateral limb as a template is shown in Figure 2; the surgeon must rely on experience and anatomical knowledge if there is a bilateral deformity. Mathematical representations of the plan were saved for subsequent steps.

B: Intraoperative phase

B4: *Mount frame*. The surgeon mounted the frame to the patient using either the chronic deformity correction or rings-first method. Unlike conventional technique, it was not necessary to accurately mimic the shape of the deformity unless the surgeon wished to compare the final correction schedule against the correction schedule computed using the conventional technique. The surgeon was free to use any combination of Kirschner wires and Steinman pins to mount the frame.

B5: *Patient registration*. A tracked coordinate reference frame (CRF) was rigidly mounted to the target anatomy. The surgeon used a tracked sharp stylus to digitize, or collect data from, the surface of the bone, typically 20 or fewer. A robust registration algorithm was used to estimate the transformation from patient coordinates to the preoperative CT coordinates (17).

B6: *Locate rings*. The surgeon digitized the fiducial landmarks on each ring. These points were used to register computer models of the rings to the actual Ilizarov rings that were attached to the patient.

B7: *Calculate initial strut lengths*. The initial length of each strut was computed as the distance between corresponding end points, using the location of each ring known from the previous step. This provided a useful intraoperative validation of the procedure
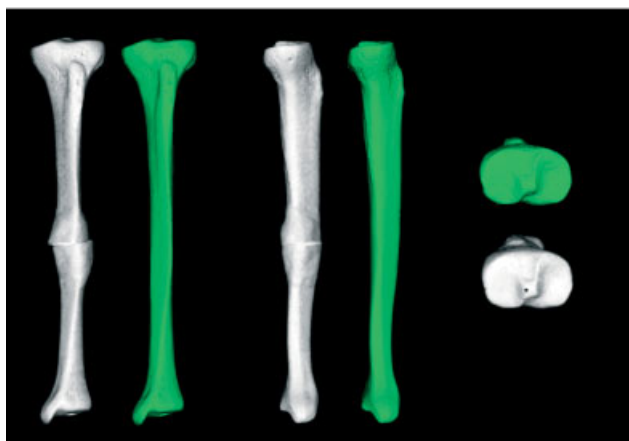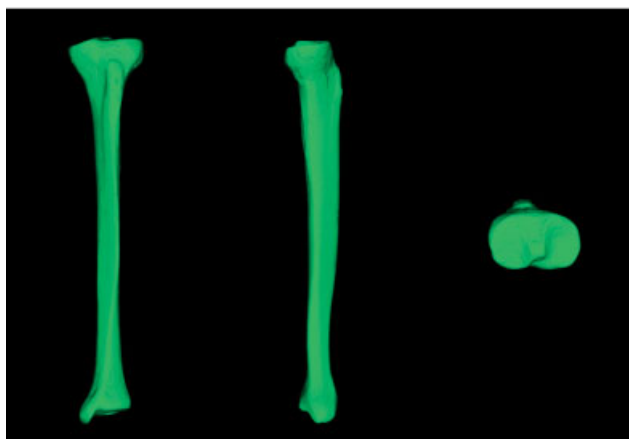
Figure 2. Planning the correction of a deformed tibia. (Top) A deformed left tibia shown in the standard anatomical reference planes. (Middle) A normal tibia used as a template to guide the correction of the deformed tibia. The surgeon must rely on knowledge of anatomy and experience if the contralateral limb cannot be used as a template. (Bottom) A virtual osteotomy was performed and the proximal end of the deformed tibia was manipulated to restore the bone to normal anatomical alignment

because the actual strut lengths could be compared against the computed strut lengths.

C: Postoperative phase

C8: Compute correction schedule. The final strut lengths were computed by applying the planned rotation

and translation to the location of the proximal ring (in CT coordinates). The duration of the correction was computed so as to move the reference point by approximately 1 mm/day. Interpolation was used to determine the daily lengths of each strut. The surgeon examined the schedule and discussed the process with the patient.

C9: Laboratory validation. To validate our technique, additional surface points were digitized from the proximal and distal fragments. These were separately registered to the computer models, providing an actual correction that could be compared to the planned correction.

Laboratory study

We performed a study using tibial plastic models, or phantoms (Sawbones, Pacific Research Laboratories Inc., Vashon, USA). Our study was designed to simulate the clinical situation where a normal contralateral limb is available to serve as a template to plan the correction. Our apparatus consisted of: an Optotrak 3020 optical tracking system (Northern Digital Inc., Waterloo, Canada); a coordinate reference frame (CRF) attached to the proximal end of the tibia phantom; a tracked surgical stylus; 15 phantoms of deformed tibias (Figure 3); and one phantom of a normal tibia.

For each phantom, a 3D surface model was constructed from CT data. Planning software was used to plan a correction for each phantom. The plan for each of the 15 deformed phantoms was to correct the deformity. A corresponding normal, undeformed phantom was available for 10 of the tibias; the normal tibia was used to define the template for the ground truth correction. The magnitude of the deformity was specified by the manufacturer for the remaining five tibias; the templates for the ground truth corrections were based on this information. We also attempted arbitrary displacements of the unaffected distal end using four of the phantoms.

Figure 3. The three types of deformed phantoms used in our laboratory study. Approximate deformities were: (left) 10° valgus with 30° internal rotation; (middle) oblique deformity 15° varus with 10° procurvatum; (right) 30° varus
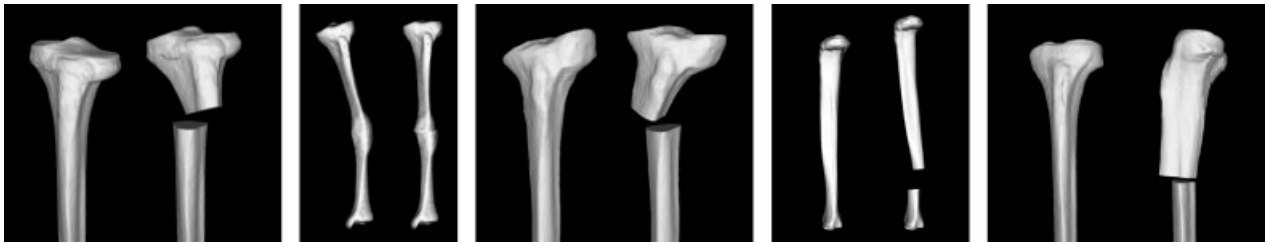
Figure 4. Examples of planned corrections used in the laboratory study. The three left-most images show examples of corrections of deformed phantoms. The fourth image shows an example of a primarily lengthening displacement on the distal end. The last image shows the 75° axial rotation displacement using the normal phantom

We attempted a 75° axial rotation displacement using the normal phantom. Examples of the planned corrections are shown in Figure 4.

The Taylor spatial frame was mounted to the bone phantom using Kirschner wires and Steinman pins. We did not attempt to exactly mimic the shape of the deformity when mounting the frame to the phantom. The CRF was attached to the proximal end of the phantom for registration purposes after mounting the frame.

The phantom and rings were digitized and registered according to our methodology and as described more fully in the Appendix. Approximately 20 registration points were collected from the osteotomy region, as well as from other surfaces that could be easily digitized percutaneously, such as the shaft and medial malleolus of the tibia; these were registered to the computer models, as described in the Appendix. Three fiducial landmarks were digitized from each ring. The struts were assembled, with the actual lengths noted for comparison to the computed lengths. The tibia phantom was then cut and distracted by setting the lengths of the struts to the calculated final lengths.

We measured the actual correction by separately registering the distal and proximal fragments after distracting the cut phantom; the ICP algorithm (18) was used for registration purposes. Approximately 50 points distributed over the surface of the entire fragment were digitized for shape-based registration. The registration points were registered to the template model (not the model of the planned correction); thus, for the 15 deformed phantoms, our measurements included planning errors caused by failing to exactly replicate the template. As described in the Appendix, we computed the rotational and translational errors between the actual and planned corrections.

Results

All error measurements for the laboratory study are tabulated in Table 3 (rotational errors are absolute values measured in the standard anatomical planes). The worst-case rotational error had a magnitude of 4.4° and occurred when we were performing the 75° axial displacement. The worst-case lengthening error was a 3.0 mm over-correction that occurred when we were performing a primarily lengthening displacement.

In three cases we observed obvious error in registering the phantom. We repeated the registration of the phantom in each of these cases.

Preliminary clinical results

Five clinical procedures have been performed at Kingston General Hospital (Kingston, Canada) to date. We obtained ethical approval for our study from all of our affiliated institutions. We obtained informed consent from all of our patients. All of the surgeries were supervised by one of the authors (D.P.B).

The first patient presented with a proximal tibial growth-plate arrest that was secondary to a fracture; the result was a recurvatum deformity secondary to an eccentric growth arrest anteriorly (Figure 5). This deformity caused a stretch of the posterior capsule and posterior cruciate ligament that produced an unstable knee. The achieved correction, measured radiographically, was from an initial −14° to a final +7° of posterior slope. Figure 6 illustrates the mounting of the frame to the patient, patient registration and ring registration steps. Figure 7 shows the lateral intraoperative and 1 month postoperative X-ray images.

The second patient presented with a proximal tibial soft-tissue imbalance that was thought would eventually lead to a recurvatum deformity. An increase in the

Figure 5. Photograph from our first clinical case illustrating the tibial recurvatum deformity

Figure 6. Intraoperative photographs from our first clinical case. (Left) Mounting the frame to the patient. (Middle) Registration of the patient to preoperative CT coordinates. The surgeon was able to use a sharp stylus to percutaneously digitize registration points from the bony anatomy. (Right) Registration of the rings
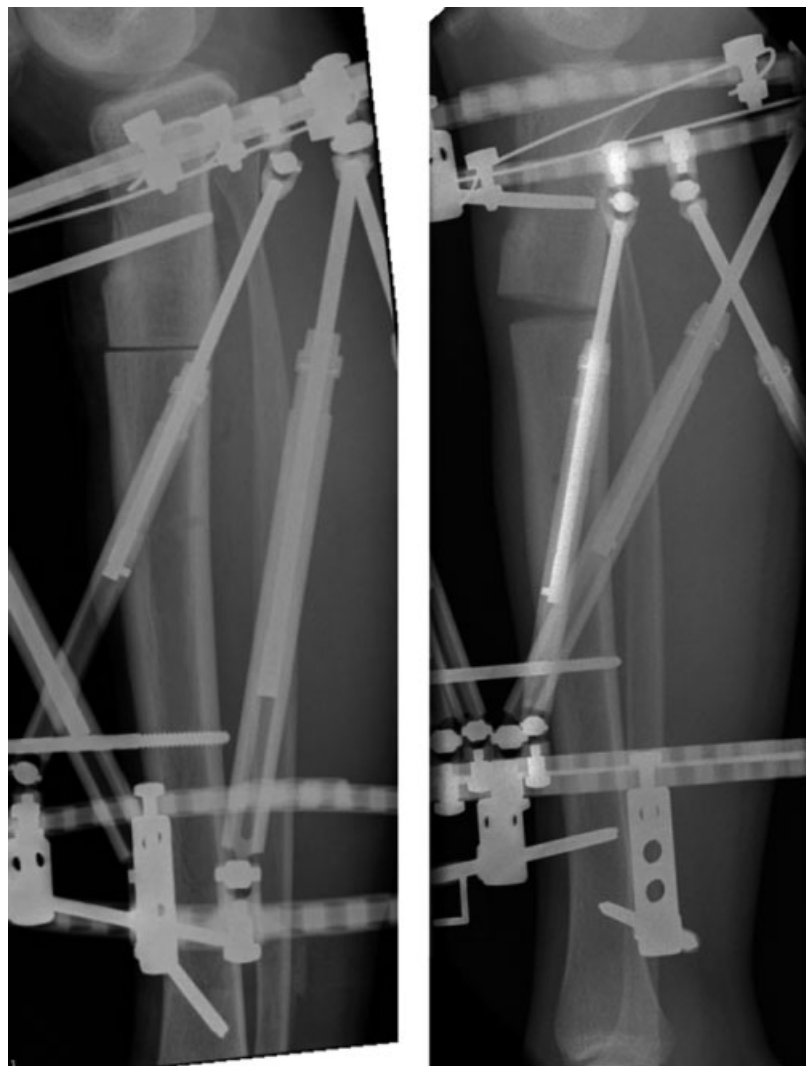

Figure 7. Intraoperative (left) and 1 month postoperative lateral X-rays from our first clinical case

posterior slope of the tibia was induced to compensate for the soft tissue deformity. The radiographic correction was an increase in posterior slope from +7° to +14° and from 5° varus to 8° varus.

The third patient presented with a partially-healed malunited tibial fracture with 14° of proximal tibial varus and 16° of posterior slope. In spite of an uncomplicated frame application, the patient was not compliant with postoperative care and the frame was removed before correction could be achieved.

The fourth patient had a 3.2 cm leg length discrepancy secondary to fibular hemimelia. His associated foot deformity exacerbated the leg length discrepancy. His tibia was lengthened by 4 cm and an increase in the posterior slope of the tibia was induced in order to compensate for a deficient anterior cruciate ligament.

The fifth patient presented with a 20° external rotation deformity of his femur that was affecting his gait. He also had an incidental 3° valgus deformity of the femur. His rotation was corrected to a neutral foot axis, which improved his gait, and the 3° valgus deformity was corrected concomitantly.

Discussion

In the laboratory validation, the largest rotational error occurred when we attempted the 75° axial rotational displacement of the normal phantom. The final configuration of the frame was very unusual in this case because we were simulating a deformity rather than a correction. We found that the frame had a noticeable rotational laxity about its vertical axis in its final configuration that contributed to the measured axial rotation error of 4.2°. In the other cases, significant frame laxity was not observed, and we speculate that the two most significant sources of error were registration error of the bone (step B5) and frame (step B6). Because we did not have access to engineering drawings of the frame, our model of the strut end points (Table 1) may also contain some small errors that would contribute to the frame registration error. We do not believe that loss of tension in the mounting struts and wires was a significant source of error in our laboratory study.

We have demonstrated that our technique is able to achieve high accuracy and precision in a laboratory setting, and that it achieved clinically acceptable outcomes in a small pilot study. Our method has additional desirable features.

The intraoperative registration of the patient and the rings effectively measured the 3D geometric relationship of the rings to the patient. Knowledge of the geometric relationship eliminated the need to radiographically measure the four parameters describing the location and axial rotation of the reference bone fragment relative to the reference ring, and the surgeon was no longer required to mount the frame so that it mimicked the deformity. Freedom in positioning the rings is clinically useful because incorrectly positioned rings do not need to be remounted and rings can be repositioned if necessary to eliminate awkward strut configurations. Our method is essentially a computer-assisted version of the conventional total-residual-deformity correction method.

Our technique has some limitations. We required a preoperative CT scan that would not be required when using conventional technique. The additional dose of ionizing radiation from the CT scan may not be acceptable to some surgeons and patients; note, however, that we did not require intraoperative fluoroscopy to check the alignment of the rings. The reported technique relied on 3D models that must be segmented from the CT scan and imported into customized planning software. Intraoperatively, a tracking system was required to perform the necessary registrations of the patients and rings.

This technique is a considerable advance over our previous efforts to navigate the fixation pins that hold the rings to the patient (14). Navigating pin placement is possible when using plastic phantoms, but we found it much more difficult to do so in clinical practice. The main reason for this was that the pin placement had to be preoperatively planned, but intraoperative conditions, such as the positioning of the patient or unforeseen soft-tissue constraints, made it impractical to carry out the plan. Furthermore, it is not easy to navigate the thin, flexible Kirschner wires that some surgeons prefer to use for ring fixation. One advantage of navigating the ring placement is that the rings could be navigated into the conventional placement; the conventional frame parameters could then be computed and the conventional software used to compute the correction schedule. Surgeons might feel more comfortable using a navigated system that produces the conventional end result of a neutral frame configuration.

We used a straightforward percutaneous shape-based registration for the patient-to-CT registration. In laboratory experiments, our registration algorithm produced median rotational registration errors of 2–3° (17); such registration errors will affect the final correction. It would be possible to use other modalities, such as fluoroscopy or ultrasound, to perform the registration. Such modalities might be preferable to our approach, especially on anatomy that cannot be easily digitized percutaneously. We observed obvious registration failures in our laboratory study; as with all computer-assisted procedures, the surgeon must be ever mindful of the possibility of registration failure.

There is an intriguing extension of our method that could also be useful: we believe that it may be possible to perform a computer-assisted Ilizarov procedure by using only a postoperative CT scan of the frame and the limb on which it is mounted. The 3D relationship of the rings relative to the patient and a postoperative planned correction could be determined from the postoperative CT scan; this would provide sufficient information to compute an appropriate correction schedule. The rings of the Taylor spatial frame, being made of aluminium, would not cause significant degradation of the CT images, although the stainless steel pins and wires might make imaging of the bony anatomy difficult. The advantages of this extension would be that it would retain all of the desirable features of our current method and eliminate the need for intraoperative registration and navigation.

Table 1. Strut end points for 180 mm diameter rings

Proximal ring	Distal ring
$(109.5, 0 - 6.67°, -16)$	$(109.5, 300 + 6.67°, 16)$
$(109.5, 0 + 6.67°, -16)$	$(109.5, 60 - 6.67°, 16)$
$(109.5, 120 - 6.67°, -16)$	$(109.5, 60 + 6.67°, 16)$
$(109.5, 120 + 6.67°, -16)$	$(109.5, 180 - 6.67°, 16)$
$(109.5, 240 - 6.67°, -16)$	$(109.5, 180 + 6.67°, 16)$
$(109.5, 240 + 6.67°, -16)$	$(109.5, 300 - 6.67°, 16)$

Results of a preliminary laboratory study (19) suggest that the extension may also be clinically useful.

Conclusion

We have presented an approach for Ilizarov's method with the Taylor spatial frame that uses preoperative CT scanning and intraoperative navigation. In our laboratory study using plastic phantoms, we measured angular and lengthening errors no larger than 4.4° and 3.0 mm, respectively. We have successfully tested our methods in a small clinical pilot study.

Appendix

We represented points and transformations in homogeneous coordinates. A point $\mathbf{q}$, located in the patient-coordinate frame, was represented by a column vector:

$$\mathbf{q} = \begin{bmatrix} q_x \\ q_y \\ q_z \\ 1 \end{bmatrix}.$$

If $\mathbf{q}$ was transformed from the patient frame to another frame (say, frame A), the point's coordinates in frame A were computed, using the rigid transformation $\mathbf{T}_A$, as:

$$\mathbf{q}^A = \mathbf{T}_A\mathbf{q} = \begin{bmatrix} \mathbf{R} & \mathbf{t} \\ \mathbf{0} & 1 \end{bmatrix}\mathbf{q}$$

where $\mathbf{R}$ is a 3×3 rotation matrix and $\mathbf{t}$ is a 3×1 translation vector.

This Appendix provides further mathematical details of the steps given in Materials and methods, above.

Step A3: Preoperative planning. The surgeon performed a virtual osteotomy by selecting a plane at which the bone model will be cut. The surgeon then selected a point $\mathbf{x}_{ref}$ that was the reference point for the distraction procedure; typically, $\mathbf{x}_{ref}$ was chosen as the point in the middle of the bone on the plane of the osteotomy. Our convention was to locate the reference on the distal model fragment.

The surgeon then rotated and translated the proximal fragment to plan the desired correction. The software computed the net result of all the actions as the transformation matrix $\mathbf{T}_{plan}$, which was the transformation of the distal fragment relative to the proximal fragment as measured in the CT coordinate system.

Step B5: Patient registration. The patient-coordinate frame was located and orientated by a coordinate reference frame (CRF), which is a device that can be tracked in 3D by a tracking system. Because this frame was more or less arbitrary, we use a registration to transform points from the patient-coordinate frame to the CT-coordinate frame (the frame in which planning and visualization were performed).

Registration proceeded by the collection of a small number of points $\mathbf{r}_i$. The points were collected by touching a tracked sharp stylus on distinctive bony anatomy and served to initialize the registration algorithm. Additional points, usually fewer than 20, were collected to refine the process. The algorithm used the CT model of the patient and the collected points to estimate the rigid transformation $\mathbf{T}_{reg}$ that took any point $\mathbf{q}$ from patient coordinates to CT coordinates as:

$$\mathbf{q}^{CT} = \mathbf{T}_{reg}\mathbf{q}$$

Details of the registration algorithm were presented by Ma and Ellis (17).

Step B6: Locate rings. The guidance software used computer models of the Taylor rings to find the locations of the actual rings (these models can be derived from manufacturer specifications or by empirical reconstruction). Distinctive fiducial points on the actual rings corresponded to specific points on the computer models.

The surgeon used a tracked sharp stylus to collect fiducial points on the actual rings; these points were measured in patient coordinates. The model of the proximal ring was registered to the actual ring using the fiducial points $\{F_p\}$, giving the transformation $\mathbf{T}_p$. Similarly for the distal ring, fiducial points $\{F_d\}$ yield the transformation $\mathbf{T}_d$. This type of registration can be performed using any absolute-orientation solver, such as Horn's method (20).

For the rings of 180 mm diameter, Figure 8 illustrates the rings, fiducial landmarks, and end points of the struts. Table 2 specifies the fiducial landmarks numerically in cylindrical coordinates (radius, angle, z), where the radius
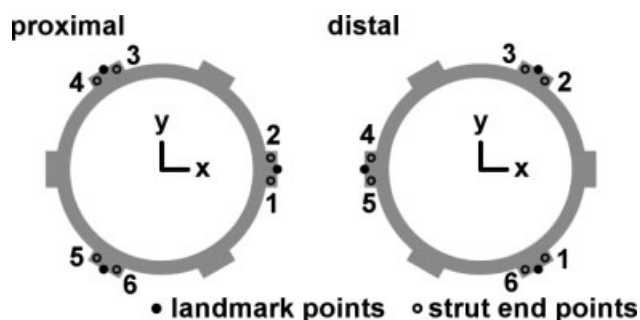

Figure 8. Proximal and distal ring models of 180 mm diameter, showing fiducial landmarks and strut end points

Table 2. Fiducial landmarks for 180 mm diameter rings

Proximal ring	Distal ring
(116.4, 0°, 0)	(116.4, 0°, 0)
(116.4, 120°, 0)	(116.4, 180°, 0)
(116.4, 240°, 0)	(116.4, 300°, 0)

Table 3. Rotational and lengthening errors measured in the laboratory study

	Rotation (°)				Length (mm)
	Coronal	Sagittal	Transverse	Total	
Value (correction of deformity)	0.8	0.2	0.2	0.8	−0.7
	1.0	0.4	1.2	1.6	3.0
	0.2	0.9	0.3	0.9	2.8
	1.5	0.8	3.7	1.7	0.6
	1.2	2.1	0.0	2.4	−2.0
	2.0	2.6	0.5	3.3	0.2
	0.3	0.1	0.7	0.8	0.1
	0.5	1.0	1.4	1.8	0.7
	1.6	0.2	1.2	2.0	−2.5
	0.2	0.4	1.1	1.2	1.3
	0.8	0.7	1.3	1.8	−0.5
	0.7	0.2	0.4	0.8	0.6
	0.4	0.9	0.4	1.0	0.2
	0.3	2.0	2.4	2.7	0.7
	0.1	0.0	1.6	1.7	−0.7
	0.2	1.3	0.9	1.4	0.3
Value (simulated deformity)	2.2	0.1	0.7	2.3	1.0
	0.6	0.2	1.2	1.4	0.9
	1.3	0.1	1.4	1.9	−1.6
	1.2	0.7	4.2	4.4	1.3
Mean	0.8	0.7	1.2	1.8	0.3
Range	0.1–2.2	0.0–2.6	0.0–4.2	0.8–4.4	−2.5–3.0

and z-coordinate are in millimeters and the angle is in degrees.

Step B7: Calculate initial strut lengths. The actual length of each of the six struts was computed as the Euclidean distance between its proximal end point and its distal end point. The calculation can be done in patient coordinates or CT coordinates (length is invariant to rigid-body transformation). Table 1 gives the locations of the end points numerically in cylindrical coordinates (radius, angle, z), where the radius and z-coordinate are in millimeters and the angle is in degrees.

Step C8: Compute correction schedule. As mentioned above, the distal ring was taken to be stationary. At any time t during the correction schedule, the location of the distal strut end point $\mathbf{d}_i$, $i = 1 \ldots 6$, in CT coordinates was:

$$\mathbf{d}_{i,t}^{\mathrm{CT}} = \mathbf{T}_{\mathrm{reg}}\mathbf{T}_d \mathbf{d}_i$$

The initial location (at time $t = 0$) and final location (at time $t = n$) of the model proximal strut end point $\mathbf{p}_i$,

$i = 1 \ldots 6$, in CT coordinates were:

$$\mathbf{p}_{i,t=0}^{\mathrm{CT}} = \mathbf{I}_{4\times4}\mathbf{T}_{\mathrm{reg}}\mathbf{T}_p \mathbf{p}_i$$
$$\mathbf{p}_{i,t=n}^{\mathrm{CT}} = \mathbf{T}_{\mathrm{plan}}\mathbf{T}_{\mathrm{reg}}\mathbf{T}_p \mathbf{p}_i$$

where $\mathbf{I}_{4\times4}$ is the 4×4 identity matrix.

The number of days n was calculated from the desired correction. From the preoperative plan, the reference point $\mathbf{x}_{\mathrm{ref}}$ would be displaced to $\mathbf{T}_{\mathrm{plan}}\mathbf{x}_{\mathrm{ref}}$. If the correction included rotation, as is usually the case, the reference point would be displaced in a helical path. We used a screw decomposition to find the path, and then applied the Ilizarov convention of displacing the reference point by 1 mm/day to find the number of days n of the correction schedule. The screw displacement was also used to compute the length of each strut on each day of the correction.

A screw transformation is a rotation of angle θ about an axis with direction b passing through the point c, followed by translation of magnitude M along the same axis (21). Given a rigid-body transformation, the corresponding screw parameters can be found; similarly, given screw parameters, the corresponding rigid-body transformation $S(b, c, \theta, M)$ can be found.

We computed the schedule by interpolating between $\mathbf{I}_{4\times4}$ and the planned transformation $\mathbf{T}_{\mathrm{plan}}$ of the proximal fragment relative to the distal fragment using the screw representation of $\mathbf{T}_{\mathrm{plan}}$. At time t, the interpolated transformation was $\mathbf{T}_t$, the CT coordinates of the proximal strut end points were:

$$\mathbf{p}_{i,t}^{\mathrm{CT}} = \mathbf{T}_t \mathbf{T}_{\mathrm{reg}}\mathbf{T}_p \mathbf{p}_i$$

and the strut lengths $s_{i,t}$ were:

$$s_{i,t} = \left((\mathbf{p}_{i,t}^{\mathrm{CT}} - \mathbf{d}_{i,t}^{\mathrm{CT}}) \cdot (p_{i,t}^{\mathrm{CT}} - \mathbf{d}_{i,t}^{\mathrm{CT}})\right)^{1/2}$$

We used a discrete search over θ and M to find the strut lengths:

- Find the screw parameterized by b, c, θ, and M corresponding to $\mathbf{T}_{\mathrm{plan}}$
- Set $d\theta = \theta/N$, $dM = M/N$ for some large N (say $N = 1000$)
- Set $\mathbf{x}_{\mathrm{old}} = \mathbf{x}_{\mathrm{ref}}$
- Set $t = 1$
- For $j = 1 \ldots N$:
  ○ Set $\theta_j = j \times d\theta$
  ○ Set $M_j = j \times dM$
  ○ Set $\mathbf{T}_j = S(b, c, \theta_j, M_j)$
  ○ Set $\mathbf{x}_j = \mathbf{T}_j\mathbf{x}_{\mathrm{ref}}$
  ○ If $||\mathbf{x}_j - \mathbf{x}_{\mathrm{old}}|| \geq 1$ mm:
    ■ Compute strut lengths $S_{i,t}$ for day t
    ■ Set $t = t + 1$
    ■ Set $\mathbf{x}_{\mathrm{old}} = \mathbf{x}_j$
  ○ End if:
- End for:
- Compute strut lengths $S_{i,t}$ for the last day t

Step C9: Laboratory validation. We measured the actual correction by separately registering the distal and proximal fragments after distracting the cut phantom. Points that were distributed over the surface of the entire fragment were digitized for shape-based registration. Registration was performed using Besl and McKay's ICP algorithm (18).

The actual rigid-body transformation of the proximal fragment relative to the distal fragment, $\mathbf{T}_{\text{actual}}$, was compared to the planned displacement, $\mathbf{T}_{\text{plan}}$. The difference between the two transformations was computed as:

$$\mathbf{T}_\Delta = \mathbf{T}_{\text{plan}}(\mathbf{T}_{\text{actual}})^{-1}$$

The angle of rotation of the rotational component of $\mathbf{T}_\Delta$ was taken as the magnitude of the total angular correction error. We also measured the rotational errors projected onto the anteroposterior, lateral and axial views. The translational lengthening error was taken to be the difference in length between the corrected phantom and the planned correction of the phantom.

Acknowledgements

References

1. Beals RK, Bryant RE. The treatment of chronic open osteomyelitis of the tibia in adults. *Clin Orthop Relat Res* 2005; **433**: 212–217.
2. Feldman DS, Shin SS, Madan S, *et al*. Correction of tibial malunion and nonunion with six-axis analysis deformity correction using the Taylor spatial frame. *J Orthop Trauma* 2003; **17**(8): 549–554.
3. Lerner A, Fodor L, Stein H, *et al*. Extreme bone lengthening using distraction osteogenesis after trauma: a case report. *J Orthop Trauma* 2005; **19**(6): 420–424.
4. Taylor JC. Six-axis deformity analysis and correction. In *Principles of Deformity Correction*, Paley D (ed.). Berlin: Springer, 2002; 411–436.
5. Taylor JC. The correction of general deformities with the Taylor spatial frame fixator, 2005; http://www.jcharlestaylor.com.
6. Stewart D. A platform with six degrees of freedom. *Proc Inst Mech Eng* 1965–1966; **180**(15): (part 1,): 371–386.
7. Seide K, Wolter D, Kortmann HR. Fracture reduction and deformity correction with the hexapod Ilizarov fixator. *Clin Orthop Relat Res* 1999; **363**: 186–195.
8. Seide K, Faschingbauer M, Wenzl ME, *et al*. A hexapod robot external fixator for computer assisted fracture reduction and deformity correction. *Int J Med Robot* 2004; **1**(1): 64–69.
9. Rajacich N, Bell DF, Armstrong PF. Pediatric applications of the Ilizarov method. *Clin Orthop Relat Res* 1992; **280**: 72–80.
10. Fadel M, Hosny G. The Taylor spatial frame for deformity correction in the lower limbs. *Int Orthop* 2005; **29**(2): 125–129.
11. Slagel B, Ellis RE, Ma B, *et al*. Limb alignment correction using traditional and computer-assisted Taylor spatial frame. In *Computer Assisted Orthopaedic Surgery: Proceedings of the 7th Annual Meeting of CAOS-International; 20–23 June 2007; Heidelberg, Germany*, Langlotz F, Davies BL, Grützner PA (eds). Pro BUSINESS GmbH: Berlin, 2007; 229–230.
12. Kochs A. Computer-assisted assembly and correction simulation for complex axis deviations using the Ilizarov fixator. *Arch Orthop Trauma Surg* 1995; **114**(5): 287–291.
13. Lin H, Birch JG, Samchukov ML, *et al*. Computer-assisted surgery planning for lower extremity deformity correction by the Ilizarov method. *J Image Guid Surg* 1995; **1**(2): 103–108.
14. Iyun O, Borschneck DP, Ellis RE. Computer-assisted correction of bone deformities using a 6-DOF parallel spatial mechanism. In *Medical Image Computing and Computer-Assisted Intervention – MICCAI 2001: Proceedings of the 4th International Conference, 14–17 October 2001, Utrecht, The Netherlands*, Niessen WJ, Viergever MA (eds). Springer: Berlin, 2001; 232–240.
15. Simpson AL, Ma B, Borschneck DP, *et al*. Computer-assisted deformity correction using the Ilizarov method. In *Medical Image Computing and Computer-Assisted Intervention – MICCAI 2005: Proceedings of the 8th International Conference, 26–30 October 2005, Palm Springs (CA), USA,* Duncan JS, Gerig G (eds). Springer: Berlin, 2005; 459–466.
16. Simpson AL, Ma B, Borschneck DP, *et al*. Computer-assisted distraction osteogenesis by Ilizarov's method: a case report. *Int J Comput Assist Radiol Surg* 2006; **1**(suppl 1): 247–249.
17. Ma B, Ellis RE. Robust registration for computer-integrated orthopedic surgery: laboratory validation and clinical experience. *Med Image Anal* 2003; **7**(3): 237–250.
18. Besl PJ, McKay ND. A method for registration of 3D shapes. *IEEE Trans Pattern Anal Mach Intell* 1992; **14**(2): 239–256.
19. Ma B, Simpson AL, Ellis RE. Proof of concept of a simple computer-assisted technique for correcting bone deformities. In *Medical Image Computing and Computer-Assisted Intervention – MICCAI 2007: Proceedings of the 8th International Conference; 29 October–2 November 2007, Brisbane, Australia*, Ayache N, Ourselin S, Maeder A (eds). Springer: Berlin, 2007; 935–942.
20. Horn BKP. Closed-form solution of absolute orientation using unit quaternions. *J Opt Soc Am A* 1987; **4**(4): 629–642.
21. McCarthy JM. *An Introduction to Theoretical Kinematics*. MIT Press: Cambridge, 1990.